Elsevier Editorial System(tm) for Earth and Planetary Science Letters

Manuscript Draft

Manuscript Number:

Title: Long-period Astronomically-forced Terrestrial Carbon Sinks

Article Type: Letters

Keywords: Orbital Forcing, Magnetostratigraphy, Coals, Paleoclimate, Oligocene

Corresponding Author: Mr. Luis Valero,

Corresponding Author's Institution: University of Barcelona

First Author: Luis Valero

Order of Authors: Luis Valero; Lluís Cabrera; Alberto Sáez; Frits Hilgen; Miguel Garcés

Abstract: Sequestration of organic matter by peat accumulation constitutes a primary sink for carbon in the global carbon cycle. Assessing the processes that control the formation and storage of peat at geological time scales is a non-solved issue of fundamental importance for understanding the global climate system. We analyzed a 7 million years long terrestrial record of Late Oligocene age from the As Pontes Basin in Northern Spain, which demonstrates that minima in the 405-kyr and 2.4-Myr eccentricity cycles play a key role in peat formation. Such nodes exhibit reduced precession amplitudes, thus avoiding extremes in seasons and seasonal contrast for a prolonged period of time. In the As Pontes Basin, this orbital configuration is associated with a decrease in siliciclastic sedimentation and enhanced peat formation. Feedbacks between equilibrium landscapes and ecosystem stability will lead to a deceleration of weathering and erosion rates in catchment areas and to minimize and stabilize the sediment flux along the sediment routing system. Mid-latitude peat burial could contribute to disturb the carbon cycle by removing (atmospheric) carbon at times of minimum eccentricity.

Suggested Reviewers: Guillaume Dupont-Nivet
Université de Rennes
guillaume.dupont-nivet@univ-rennes1.fr
Paleomagnetism, Continental basins, Climate.

Luigi Jovane
Instituto Oceanográfico (Brazil)
luigijovane@gmail.com
Paleomagnetism, Cyclostratigraphy

Hemmo Abels
University of Delft
H.A.Abels@tudelft.nl
Cyclostratigraphy

Sébastien Castelltort
University of Geneva

sebastien.castelltort@unige.ch
Geomorphology, Climate and Tectonics Evolution

Antonio García-Alix
University of Glasgow
Antonio.Garcia-AlixDaroca@glasgow.ac.uk
Stratigraphy, Continental sedimentology, paleolimnology, Climate change

Opposed Reviewers:

Universitat de Barcelona

Departament d'Estratigrafia, Paleontologia i Geociències Marines

Facultat de Geologia
Martí i Franquès s/n 08028 Barcelona, Spain
Tel. (34) 93 402 13 84; Fax. (34) 93 402 13 40

Barcelona, October 29 2015

Dear Editor,

Please find attached our manuscript entitled: "Long-period astronomically forced terrestrial carbon sinks". The manuscript contains new original data and interpretations neither published nor under consideration for publication elsewhere.

In this paper we show the link between long-period orbital oscillations, development of peatlands and carbon storage. Such finding is noticeable as it focuses on processes which have an impact on the carbon cycle, of high social interest due to its relationship with climate system.

Earlier works have already established the link between wet-arid climatic shifts and coal accumulation at shorter time scales. The most remarkable aspect of this piece of work, however, is the long-term transmission mechanisms from orbital rhythms to the geological record. We propose that equilibrium landscapes and resilient vegetal cover promoted retreats of the clastic wedges during prolonged intervals of low-amplitude insolation changes. The reduction of terrigenous sediments allowed peat development and eventually carbon storage.

Because of its multi-disciplinary approach and the implications for Earth's climate system, we consider this work significant and of broad interest for the Earth Sciences community. For this reason we consider *Earth and Planetary Science Letters* the appropriate journal for publishing this work.

We provide a manuscript of about 4500 words and six figures, three of them in colour.

Looking forward to hearing from you. Sincerely,

Luis Valero

Universitat de Barcelona

Departament d'Estratigrafia, Paleontologia i Geociències Marines

Facultat de Geologia
Martí i Franquès s/n 08028 Barcelona, Spain
Tel. (34) 93 402 13 84; Fax. (34) 93 402 13 40

Corresponding author:

Luis Valero

Depart. Estratigrafia, Paleontologia i Geociencies Marines, Facultat de Geologia

Martí i Franquès s/n E-08028 Barcelona, Spain

Email: **luisvalero@ub.edu**

Co-authors

Frederik Hilgen, F.J.Hilgen@uu.nl, ***Affiliation:*** Department of Earth Sciences, Utrecht University, Heidelberglaan 2, 3584 CD Utrecht, The Netherlands

Miguel Garcés, mgarces@ub.edu

Lluís Cabrera, lluis.cabrera@ub.edu

Alberto Sáez, a.saez@ub.edu

Affiliation

Grup de Geodinàmica i Anàlisi de Conques (GGAC), Institut de Recerca GEOMODELS.

Departament d'Estratigrafia, Paleontologia i Geociències Marines, Facultat de Geologia, Universitat de Barcelona, Martí i Franquès s/n, 08028-Barcelona, Spain

Suggested Reviewers

Guillaume Dupont-Nivet, Université de Rennes (France), guillaume.dupont-nivet@univ-rennes1.fr, Paleomagnetism, Continental basins, Climate.

Luigi Jovane, Instituto Oceanográfico (Brazil), Paleomagnetism, Cyclostratigraphy

Hemmo Abels, University of Delft (Netherlands), H.A.Abels@tudelft.nl. Cyclostratigraphy

Sébastien Castelltort, University of Geneva (Switzerland), sebastien.castelltort@unige.ch. Geomorphology, Climate and Tectonics Evolution.

Antonio Garcia-Alix, Glasgow University (UK), Antonio.Garcia-AlixDaroca@glasgow.ac.uk, Stratigraphy, Climate change.

***Highlights (for review)**

Coal accumulation is paced by the 2.4-Myr and 405-kyr eccentricity cycles

Reduced clastic input allowed carbon accumulation during eccentricity minima

Low precession amplitude times promoted vegetation cover and equilibrium landscapes

Peat burial contribute to remove carbon at times of minimum eccentricity

1 *Long-period Astronomically-forced Terrestrial Carbon Sinks.*

2 *Luis Valero[1], Lluís Cabrera[1], Alberto Sáez[1], Frits Hilgen[2], Miguel Garcés[1]*

3 1. *GEOMODELS Institute, Departament d'Estratigrafia, Paleontologia i Geociències*
4 *Marines, Facultat de Geologia, Universitat de Barcelona, Martí i Franquès s/n, 08028*
5 *Barcelona, Spain.*
6 2. *Department of Earth Sciences, Utrecht University, Heidelberglaan 2, 3584 CD Utrecht,*
7 *The Netherlands*

8 ***Abstract***

9 Sequestration of organic matter by peat accumulation constitutes a primary sink for carbon in
10 the global carbon cycle. Assessing the processes that control the formation and storage of peat
11 at geological time scales is a non-solved issue of fundamental importance for understanding
12 the global climate system. We analyzed a 7 million years long terrestrial record of Late
13 Oligocene age from the As Pontes Basin in Northern Spain, which demonstrates that minima in
14 the 405-kyr and 2.4-Myr eccentricity cycles play a key role in peat formation. Such nodes
15 exhibit reduced precession amplitudes, thus avoiding extremes in seasons and seasonal
16 contrast for a prolonged period of time. In the As Pontes Basin, this orbital configuration is
17 associated with a decrease in siliciclastic sedimentation and enhanced peat formation.
18 Feedbacks between equilibrium landscapes and ecosystem stability will lead to a deceleration
19 of weathering and erosion rates in catchment areas and to minimize and stabilize the sediment
20 flux along the sediment routing system. Mid-latitude peat burial could contribute to disturb
21 the carbon cycle by removing (atmospheric) carbon at times of minimum eccentricity.

22 ***Introduction***

23 Very long-term orbital oscillations (>1Myr) play an important role as triggers of irreversible
24 changes of past climates (Zachos et al., 2001). Studies of long-period cycles as recorded in

continental sediments are essential to disentangle the local, regional and global importance of the associated climate changes (e.g. Abels et al., 2012). The search of these cycles in continental basins is, however, particularly challenging because of their inferred low preservation potential. Basic requirements for their development and study are stability of the basin depositional setting, sensitivity of the sedimentary environment to climate variations, and the preservation of a long stratigraphic record that preferably spans several cycles. A limited number of case studies exist that fully document long-period cyclicity in lacustrine systems (Olsen and Kent, 1999; Kashiwaya et al., 2001, Abels et al., 2010a; Valero et al., 2014). However, recent studies show that these cycles can also be recognized in apparently less favourable continental settings such as fluvial systems (Abels et al., 2013; Hilgen et al., 2014), and that million-year scale climatic cycles can occur superimposed on the longterm tectonic signature of foreland basins (Valero et al., 2014). These results should stimulate debate on the various forcing factors that control sedimentation in different continental basins (Shanley and McCabe, 1994) and on different timescales at which they operate (Miall, 2014).

Available numerical climate models help to understand the sedimentary system response to climate change related to the short-period cycles of precession and obliquity (e.g., Bosmans et al., 2014). However, considerable uncertainty remains on the forcing mechanisms at million-year time scales such as that of the very long-period eccentricity cycle. Agreement exists in that the alteration of the hydrological cycle, summarized as the balance between precipitation and evaporation must exert a prime control on sedimentary cyclicity. Nevertheless, climate can affect depositional settings through other processes, namely via their impact on vegetation cover, sediment production and (ground) water chemistry. In addition, sedimentary facies distribution is sensitive to erosional patterns in the catchment basin and the dynamics of sediment transfer systems, both intimately linked to vegetation cover and the morphology of the basin.

To understand how climate, by means of the million year-scale orbital oscillations, affects the sediment routing system and sedimentary facies distribution, we focused on a long coal-bearing stratigraphic record. Increase of clastic supply can lead to shrinking and obliteration of peatlands, thus making these systems excellent indicators of changes in vegetation and erosion in the catchment basin. Precession, obliquity and short eccentricity-related orbital forcing of coal-bearing sequences has already been documented (van Vugt et al., 2001; Large et al., 2003; Large et al., 2004; Briggs et al., 2007), and further correlated to marine climatic records (van Vugt et al., 1998). However, compelling evidence for a relationship between coal formation in mid-latitude swampy environments and long-period Milankovitch cycles has not yet been found. As peatlands are significant contributors to the carbon cycle (Large et al., 2004), understanding the climatic controls on coal formation is critical to better understand forcing and feedbacks in Earth's climate system.

In this paper, a cyclostratigraphic analysis of the Upper Oligocene coal-bearing sequence of the As Pontes Basin in NW Spain is carried out. The long time span of *ca.* 7 Myr of this record was essential for the investigation of recurrent basin-wide coal expansions. Magnetostratigraphic data from earlier studies (Huerta et al., 1997) were revised and integrated in this study in order to provide the necessary temporal framework. Spectral analysis was applied on selected borehole data with the aim to statistically test the orbital forcing hypothesis of the sedimentary cyclicity, before comparing the cycle record with orbital target curves. The significance of the cyclicity and the mechanisms through which insolation changes that result from Earth's orbital geometry are transmitted to the sedimentary record are discussed.

Geological setting and section/cores

The As Pontes Basin developed along a NW-SE-oriented dextral strike-slip fault system associated with the convergence between the Iberian and European plates (Santanach et al., 2005). The northern basin margin is structurally complex, characterized by a vertical stack of

numerous southward directed thrusts sheets coeval with N-S directed extensional faults derived from the major fault system (Fig. 1). The basin is divided into two fault-bounded sub-basins and the basin infill consists of a 400 m thick coal-bearing sedimentary record. A detailed basin stratigraphy is based on high-resolution basin-wide correlations, using the core database of the mining company. The bedrock of the catchment area consists mostly of Paleozoic slate and Precambrian meta-graywackes. Small-sized alluvial fan deposits accumulated in the proximal areas, and interfinger basinwards with metric and decametric-scale peat deposits (Fig. 2). Shifts of the facies belts led to the organization of the sedimentary fill into basin-wide decameter-scale sequences. Such sequences consist of a coal-rich clayey lower unit overlain by a clastic unit, which was mainly fed from alluvial fans along the northern basin margin (Fig. 2, Fig. 3). This cyclic stacking pattern is interrupted by a major clastic episode (Middle Sandstone Unit) in the middle of the sequence, which marks the complete connection between the two sub-basins during the late stage of the basin fill. The Middle Sandstone Unit onlaps on the structural high bounding the western and eastern sub-basins, and is associated with a rearrangement of the alluvial network following the connection of the sub-basins (Ferrús, 1998). Cyclic aggradation of the coal/clastic sequences is resumed after this episode. Finally, basin overfilling is marked by a coarsening trend, representing alluvial progradation due to a reduction of the accommodation space.

The paleobotanical record suggests a semitropical swamp forest environment (Cavagnetto, 2002), where warm and humid conditions prevailed in a continental non-ombrotrophic peatland. Faunal remains are scarce, but the occurrence of the fossil rodent *Issiodoromys minor* (López-Martínez et al., 1993) at the base of the West section provides a biochronological constraint, suggesting a correspondence with the MP24 mammal reference level (upper Rupelian; Gradstein et al., 2012). A magnetostratigraphic study of the complete record provided a preliminary correlation to the polarity time scale (Huerta et al., 1997). For our study

100 we used the West section of Huerta et al. (1997) and six cores located in the center of the
101 western sub-basin of the As Pontes basin (see Fig. 1 for localities).

102 ***Magnetostratigraphic age model***

103 The former magnetostratigraphy-based age model of Huerta et al. (1997) for the West section
104 was revisited (Fig. 3). Their magnetostratigraphic age model is largely adopted here, except for
105 the lowermost part of the section. The correlation of the basal normal magnetozone with
106 chron C10n is not followed as it results in unrealistic changes in sedimentation rate. In
107 addition, we were reluctant to use the lower two samples for magnetostratigraphic purposes,
108 because the directional data deviate significantly from the expected geocentric dipole. As a
109 result, we propose a revised correlation of the lower part of the section in which the reversed
110 magnetozone R1 corresponds to chron C10r, and the normal magnetozone N1 with chron
111 C10n. This correlation is reinforced by the occurrence of *Issiodoromys minor* in this part of the
112 composite section, which fits well with the age range of the MP24 mammal reference level
113 (López-Martínez et al., 1993; Gradstein et al., 2012). The refined magnetostratigraphy ranges
114 from the top of chron C10r (around 29 Ma in the Rupelian) to chron C6Aar.2n in the early
115 Miocene (*ca.* 21.7 Ma, East section not shown). The topmost sediments of the western sub-
116 basin correlate with chron C6Cn.3n, just below the Oligocene-Miocene boundary (Fig. 3). The
117 resultant sedimentation rates are in general low, averaging ~3 cm/kyr.

118 The new magnetostratigraphic age model proved critical for our cyclostratigraphic analysis and
119 our attempt to establish the phase-relationship of potential orbitally-driven cycles with the
120 astronomical parameters. For this purpose we established a correlation between core MP208
121 core and the West section, where magnetostratigraphic data are available, by means of
122 detailed lithological correlations of coal-beds (Fig. 4). This correlation allowed us to apply the
123 magnetostratigraphic age model to core MP208. This model was constructed using the Age

Scale tool of the Analyseries 2.08 software (Paillard et al., 1996) and the tie-points marked in Figure 4.

Cyclostratigraphy

Six cores of the Western sub-basin were selected for cyclostratigraphic analysis. Their location in the basin center was considered optimal for minimizing noise produced by tectonics and alluvial autogenic processes. Numerical values, ranging from proximal (1) to distal (8) and summarized in figure 2, were attributed to a suite of 36 different sedimentary facies described from the cores (Fig. 2; Table 1). The sedimentary model is based on criteria formulated by Sáez et al., (2002; 2003), who studied the sedimentology and the geochemistry of the basin and classified the different facies. The description of the lithofacies in the cores provided by previous studies was fully included in our model. Sampling resolution arrived at 39.1 cm following interpolation to obtain an evenly spaced depth-series. The magnetostratigraphic age model (sedimentation rates 2.5-3.5 cm/kyr) reveals that the sampling resolution fluctuates between 15.6 and 11.14 kyr in the time domain. Such values are below the Nyquist limit for precession and obliquity, but above the detection limit for all eccentricity cycles (Herbert, 1994; Meyers et al., 2008).

Spectral analysis, phase relations and astronomical tuning

Spectral analysis focused on the lower part of the basin fill in order to exclude the thick Middle Sandstone Unit from the time series, which represents a unique and at the same time aberrant interval in the record. This unit is associated with a sharp increase in sedimentation rates, and does not appear to follow the characteristic sequential arrangement of coal units. Spectral analyses of core records were carried out in the depth domain using the Analyseries software (Paillard et al., 1996) with default parameters for the Blackman-Tukey method. Subsequently, in order to correctly handle red noise, the records were also analyzed using the REDFIT software, which is based on the conventional AR(1) red noise model (Schulz and Mudelsee,

149 2000), with a rectangular window, 4000 simulations, and default HIFAC and OFAC values. The
150 spectral analyses indicate that significant peaks in the depth domain with periods between
151 15.1 m and 7.54 m occurred in all cores (Supplementary Information). A shifting average
152 sedimentation rate of 2.5-3.5 cm/kyr as inferred from the magnetostratigraphic age model,
153 implies that these peaks centered around 12 m fall within the range of the long orbital
154 eccentricity cycle of 405-kyr.

155 Analyseries was also used to apply a Gaussian band-pass filter (frequency: 0.0827 cycles/m;
156 bandwidth: 0.05) to the MP208 core data in the stratigraphic domain to extract the cyclicity
157 with a period around of 12 m (Fig. 4). We used a wide filter, in order to include all the potential
158 cycles taken the variability in sedimentation rates into account. In addition, the use of a wide
159 filter prevents the generation of artificial amplitude modulations in the range of eccentricity
160 (Zeeden et al., 2015). On the other hand, a 405-kyr centered filter was applied to the MP208
161 core in the (magnetostratigraphic) time domain. A correlation between the maxima of these
162 filters was performed, and extended to the 405-kyr eccentricity curve (Fig. 4). We used the
163 La2004 solution for eccentricity (Laskar et al., 2004), which for this time interval is stable and
164 identical to the La2011a solution (Laskar et al., 2011). The only tuning option in which the
165 magnetostratigraphic calibration is respected reveals a phase relationship in which the clastic
166 peaks correlate with maxima in the eccentricity curve (Fig. 4).

167 The same Gaussian band-pass filter was applied to the rest of the core data, improving the
168 correlation between the cores, and enabling an astronomical tuning to the 405-kyr eccentricity
169 component for all the cores (Fig. 5). To confirm orbital forcing at a 405-kyr-scale, independent
170 of the magnetostratigraphic age model, the astronomically-tuned age model to 405-kyr
171 eccentricity was applied to the raw data for spectral analysis. The spectra reveal peaks in the
172 100-kyr band (Fig. 6), thus providing independent evidence that the 405-kyr cycle age model is
173 meaningful and that the cycles are astronomically-forced. The statistical confidence of the 100-

kyr peak is at the 95% level in two out of the five core records, and at 90 % in the other three. The enhancement of peaks in the 100-kyr cycle range after the age model refinement indicates that the facies shifts were related to eccentricity cycles. This confirms that the regular decametric clastic units are associated with 405-kyr maxima, while coal units correspond to 405-kyr eccentricity minima. Although the spectral analyses reveal 100-kyr eccentricity-forced cycles, these cycles are not consistently present throughout the entire time-series. Low sedimentation rates and low resolution in the core description data, could explain the apparent lack of sensitiveness to the 100-kyr cycle in parts of the record.

Apart from the 405-kyr eccentricity cycle forcing, the astronomical correlation highlights that the three major basin-wide lignite units, indicated in Fig. 5 as H, A-B-C, and β horizons, occur during minima of the 2.4-Myr eccentricity cycle. These units contain the thickest coal seams, with isochronal limits that can be unequivocally traced across the basin, representing the main exploitable targets for the mining company.

It is noteworthy that these cycles are found in the distal part of a setting where tectonics and autogenic processes are potentially distorting the cyclicity. Episodes of tectonic deformation and uplifting can alter both the transport routing systems and the sediment fluxes (Armitage et al., 2013). The siliciclastic progradation of the Middle Sandstone Unit may well represent the sedimentary response to a tectonic reorganization, which temporarily disturbed the cyclic arrangement. Steady uplift rates, due to shortening accommodated by numerous minor thrusts (Santanach et al., 2005), could account for the low influence of tectonics on higher-frequency sedimentary architecture in the central parts of the basin.

Orbital forcing: climatic stability and coal accumulation.

Sharp basin-wide alternations of coal seams and siliciclastic sediments occur on a 405-kyr pacing, which suggests that coal accumulation is, on first order, dictated by favourable climatic conditions related to orbital eccentricity. The recurrent progradation of the sandstone units is

associated with an increase in sedimentation rate (Fig.2). The lack of a central lake with fluctuating base level implies that these sedimentary cycles are not accommodation-forced (Valero et al., 2015). Altogether this suggests that the cycles on this time scale are driven by changes in sediment input rate. Periods of 405-kyr eccentricity maxima mark pulses of increasing clastic supply and alluvial progradation, while at times of eccentricity minima clastic supply is reduced, favouring swamp development and peat accumulation.

Eccentricity itself does not provide significant insolation differences as to modify climatic patterns, but is a modulator of precession (Berger et al., 1992; Laskar et al., 2004). During eccentricity maxima, precession extremes can lead to insolation differences of about 20% (Laskar et al., 2004; Abels et al., 2013). Favourable conditions for peat formation would occur at times of eccentricity maxima in case the periodic development of swampy peats would be controlled by maxima in the range of seasonal insolation associated with climatic precession. The reason for this is that eccentricity determines the precession amplitude and thus the range of seasonal insolation and the climatic response. However, this is in contradiction with the observation that the major coal seams occur preferentially at times of eccentricity minima. Consequently, the lack of peatlands during eccentricity maxima suggests that other factors controlled coal accumulation. Prolonged intervals marked by low-amplitude insolation changes during combined eccentricity minima of the 100-kyr and 405-kyr cycles span several tenths of thousands of years, sustaining relatively stable climatic periods that avoid extreme seasonal signals. We propose that these stable climatic conditions during eccentricity minima promoted that peatlands and their adjacent ecosystems fixed soils efficiently, thereby decreasing erosion of the surrounding reliefs (Corenblit et al., 2011). In turn, the resultant reduction in clastic sediment supply favoured peat expansion in the basin. Conversely, during eccentricity maxima, and therefore high-amplitude precession, extreme maxima in seasonality during precession minima (for the Northern Hemisphere) will lead to the shrinking and fall of ecosystems and peatland decline.

Under stable climatic conditions and enhanced vegetation cover, the basin slope tends to reach dynamic equilibrium, particularly in a very low-gradient continental basin. Geomorphologic stability also contributes to reduce erosional rates, and subsequently sediment input (Whipple, 2001; Castelltort and Van Der Driessche, 2003). These periods of stability are more pronounced during the 2.4-Myr eccentricity minima, especially when such minima are combined with minimum eccentricity associated with the 405-kyr and 100-kyr cycles. During these orbital configurations, climatic stability can persist for about 50-60-kyr. The astronomical correlation shows that it is during these periods that the thicker peat layers that cover almost the entire basin accumulated.

Coal beds constitute an important sink for carbon storage. In this case, coal deposition and thus the carbon storage phase is associated with eccentricity minima. In contrast, in the neighbouring Ebro Basin, it has been shown that lake expansion and enhanced carbonate accumulation occurred during eccentricity maxima during the same time interval (Valero et al., 2014). As carbonate accumulation in lakes constitutes another efficient carbon sink (Sobek et al., 2009), the anti-phase behaviour of the respective carbon sinks within the same climatic belt and in nearby continental basins is noteworthy. The different sedimentary response of these basins to the same climatic changes likely depends on the different characteristics of the basins. This difference in response to climate changes as a function of basin characteristics is remarkable, as is the potential for nearby basins to buffer changes in carbon storage and, thus, the global carbon cycle, associated with eccentricity cycles, even when these basins are located within the same climatic belt.

Conclusions

The good to excellent correlation between the coal-alluvial sequences in the As Pontes Basin and the 405-kyr and 2.4-Myr eccentricity cycles suggests that these sequences are controlled by orbital climate forcing. Orbital rhythms were transmitted to the sediment record by the coupling between stable and favourable climate conditions, equilibrium landscapes, and the enhanced vegetation cover resilience. This suggests that even in small-sized tectonically active settings, the climatic signature can be detected, even when it is not driven by changes in the water balance, as in lakes. If the relationship between peatlands and long-term orbital forcing is shared with other mid-latitude basins, a wide-range of sensitive environments needs to be considered as potential carbon sinks. Depending on the overall response of basins to climatic changes as a function of their physiognomy it may constitute a long-term agent of global cooling.

Acknowledgments.

This is a contribution to the ESF Research Networking programme EARTHTIME-EU. This research was funded by the Spanish projects CGL2010-17479 and CGL2014-55900-P and the Research Group of "Geodinàmica i Anàlisi de Conques" (2009GGR 1198). LV thanks the University of Barcelona for the financial support (APIF-UB) and Christina Riesselman and the University of Otago in New Zealand for providing a place to write the first parts of this article.

References

Abels, H. A., Clyde, W.C., Gingerich, P.D., Hilgen, F.J., Fricke, H.C., Bowen, G.J., and Lourens, L.J., 2012, Terrestrial carbon isotope excursions and biotic change during Palaeogene hyperthermals: Nature Geoscience, v. 5, no. 5, p. 326–329, doi: 10.1038/ngeo1427.

Abels, H. A., Kraus, M.J., and Gingerich, P.D., 2013, Precession-scale cyclicity in the fluvial lower Eocene Willwood Formation of the Bighorn Basin, Wyoming (USA): Sedimentology, v.60, p. 1467-1483, doi: 10.1111/sed.12039.

Armitage, J.J., Dunkley Jones, T., Duller, R. A., Whittaker, A.C., and Allen, P. A., 2013, Temporal buffering of climate-driven sediment flux cycles by transient catchment response: Earth and Planetary Science Letters, v. 369-370, p. 200–210, doi: 10.1016/j.epsl.2013.03.020.

Berger, A, Loutre, M.F., and Laskar, J., 1992, Stability of the Astronomical Frequencies Over the Earth's History for Paleoclimate Studies: Science, v. 255, p. 560–566, doi: 10.1126/science.255.5044.560.

Bosmans, J.H.C., Drijfhout, S.S., Tuenter, E., Hilgen, F.J., Lourens, L.J., 2014, Response of the North African summer monsoon to precession and obliquity forcings in the EC-Earth GCM: Climate Dynamics, 1-19, doi: 10.1007/s00382-014-2260-z.

Briggs, J., Large, D. J., Snape, C., Drage, T., Whittles, D., Cooper, M., Macquaker, J.H.S, Spiro, B. F., 2007. Influence of climate and hydrology on carbon in an early Miocene peatland. Earth and Planetary Science Letters, 253(3), 445-454.

Castelltort, S., and Van Den Driessche, J., 2003, How plausible are high-frequency sediment supply-driven cycles in the stratigraphic record?: Sedimentary Geology, v. 157, p. 3–13, doi: 10.1016/S0037-0738(03)00066-6.

Cavagnetto, C., 2002. La palynoflore du Bassin d'As Pontes en Galice dans le Nord Ouest de l'Espagne á la limite Rupélien-Chattien (Oligocéne): Palaeontographica Abteilung B, p. 161-204.

Corenblit, D., Baas, A.C.W., Bornette, G., Darrozes, J., Delmotte, S., Francis, R. a., Gurnell, A.M., Julien, F., Naiman, R.J., and Steiger, J., 2011, Feedbacks between geomorphology and biota controlling Earth surface processes and landforms: A review of foundation concepts and current understandings: Earth-Science Reviews, v. 106, no. 3-4, p. 307–331, doi: 10.1016/j.earscirev.2011.03.002.

Ferrús, B., 1998, Análisis de cuenca y relaciones tectónica-sedimentación en la cuenca de As Pontes (Galícia): PhD thesis, Universitat of Barcelona, 351 p.

294 Gradstein, F.M., Ogg, J.G., Schmitz, M., Ogg, G., 2012, The Geologic Time Scale 2012 2-Volume Set:
295 Amsterdam, Elsevier.

296 Herbert, T. D., 1994, Reading orbital signals distorted by sedimentation: models and examples, in de
297 Boer, P. L., and Smith, D. G., editors, Orbital Forcing and Cyclic Sequences: Oxford, Blackwell Scientific
298 Publications, International Association of Sedimentologists, Special Publication 19, p. 483–507.

299 Hilgen, F.J., Hinnov, L. a., Abdul Aziz, H., Abels, H. a., Batenburg, S., Bosmans, J.H.C., de Boer, B., Husing,
300 S.K., Kuiper, K.F., Lourens, L.J., Rivera, T., Tuenter, E., Van de Wal, R.S.W., Wotzlaw, J.-F., et al., 2014,
301 Stratigraphic continuity and fragmentary sedimentation: the success of cyclostratigraphy as part of
302 integrated stratigraphy: Geological Society, London, Special Publications, doi: 10.1144/SP404.12.

303 Huerta, Á., Parés, J. M., Cabrera, L., Ferrús i Pinyol, B., & Sáez, A. (1997). Magnetocronología de las
304 sucesiones cenozoicas de la cuenca de As Pontes (La Coruña, Noroeste de España). Acta geológica
305 hispánica, 32(3-4), 127-145.

306 Kashiwaya, K., Ochiai, S., Sakai, H., and Kawai, T., 2001, Orbit-related long-term climate cycles revealed
307 in a 12-Myr continental record from Lake Baikal: Nature, v. 410, no. 6824, p. 71–74.

308 Large, D.J., Jones, T.F., Briggs, J., Macquaker, J.H.S., and Spiro, B.F., 2004, Orbital tuning and correlation
309 of 1.7 m.y. of continuous carbon storage in an early Miocene peatland: Geology, v. 32, no. 10, p. 873–
310 876, doi: 10.1130/G20824.1.

311 Large, D.J., Jones, T.F., Somerfield, C., Gorringe, M.C., Spiro, B., Macquaker, J.H.S., and Atkin, B.P., 2003,
312 High-resolution terrestrial record of orbital climate forcing in coal: Geology, v. 31, no. 4, p. 303, doi:
313 10.1130/0091-7613(2003)031<0303:HRTROO>2.0.CO;2.

314 Laskar, J., Robutel, P., Joutel, F., Gastineau, M., Correia, A.C.M., and Levrard, B., 2004, A long-term
315 numerical solution for the insolation: Astronomy & Astrophysics, v. 285, p. 261–285, doi: 10.1051/0004-
316 6361.

317 Laskar, J., Fienga, A., Gastineau, M., & Manche, H. (2011). La2010: a new orbital solution for the long-
318 term motion of the Earth. Astronomy & Astrophysics, 532, A89.

López-Martínez, N., Fernandez Marrón, T., Peláez-Campomanes, P., and De la Peña Zarzuelo, A., 1993: Revista Sociedad Geologica España, v. 6, p. 16–28.

Machlus, M.L., Olsen, P.E., Christie-Blick, N., and Hemming, S.R., 2008, Spectral analysis of the lower Eocene Wilkins Peak Member, Green River Formation, Wyoming: Support for Milankovitch cyclicity: Earth and Planetary Science Letters, v. 268, no. 1-2, p. 64–75, doi: 10.1016/j.epsl.2007.12.024.

Meyers, S. R., Sageman, B. B., & Pagani, M. (2008). Resolving Milankovitch: Consideration of signal and noise. American Journal of Science, 308(6), 770-786.

Miall, A. D., 2014, Fluvial Depositional Systems: New York, Springer, doi: 10.1007/978-3-319-00666-6

Olsen, P.E., and Kent, D. V., 1999, Long-period Milankovitch cycles from the Late Triassic and Early Jurassic of eastern North America and their implications for the calibration of the Early Mesozoic time-scale and the long-term behaviour of the planets: Philosophical Transactions of the Royal Society A: Mathematical, Physical and Engineering Sciences, v. 357, no. 1757, p. 1761–1786, doi: 10.1098/rsta.1999.0400.

Paillard, D., Labeyrie, L., Yiou, P., 1996. Macintosh program performs time-series analysis. Eos, Transactions American Geophysical Union, v.77, p.379

Sáez, A., and Cabrera, L., 2002, Sedimentological and palaeohydrological responses to tectonics and climate in a small, closed, lacustrine system: Oligocene As Pontes Basin (Spain): Sedimentology, v. 49, p. 1073–1094, doi: 10.1046/j.1365-3091.2002.00490.x.

Sáez, A., Inglès, M., Cabrera, L., and de las Heras, A., 2003, Tectonic-palaeoenvironmental forcing of clay-mineral assemblages in nonmarine settings: The Oligocene-Miocene As Pontes Basin (Spain): Sedimentary Geology, v. 159, p. 305–324, doi: 10.1016/S0037-0738(02)00333-0.

Santanach, P., Ferrús, B., Cabrera, L., and Sáez, A., 2005, Origin of a restraining bend in an evolving strike-slip system: The Cenozoic As Pontes basin (NW Spain): Geologica Acta, v. 3, p. 225–239.

Shanley, K.W., McCabe, P.J., 1994, Perspectives on the sequence stratigraphy of continental strata: American Association Petroleum Geologists Bulletin, v.78, p. 544–568

344 Schulz, M., and Mudelsee, M., 2002, REDFIT: estimating red-noise spectra directly from unevenly spaced
345 paleoclimatic time series: Computers & Geosciences, v. 28, no. 3, p. 421–426, doi: 10.1016/S0098-
346 3004(01)00044-9.

347 Valero, L., Garcés, M., Cabrera, L., Costa, E., and Sáez, A., 2014, 20 Myr of eccentricity paced lacustrine
348 cycles in the Cenozoic Ebro Basin: Earth and Planetary Science Letters, v. 408, p. 183–193, doi:
349 10.1016/j.epsl.2014.10.007.

350 Valero, L., Huerta, P., Garcés, M., Armenteros, I., Beamud, E., & Gómez-Paccard, M. (2015). Linking
351 sedimentation rates and large-scale architecture for facies prediction in nonmarine basins (Paleogene,
352 Almazán Basin, Spain). Basin Research. doi: 10.1111/bre.12145

353 van Vugt, N., Langereis, C.G., and Hilgen, F.J., 2001, Orbital forcing in Pliocene–Pleistocene
354 Mediterranean lacustrine deposits: dominant expression of eccentricity versus precession:
355 Palaeogeography, Palaeoclimatology, Palaeoecology, v. 172, no. 3-4, p. 193–205, doi: 10.1016/S0031-
356 0182(01)00270-X.

357 Van Vugt, N., Steenbrink, J., Langereis, C.G., Hilgen, F.J., and Meulenkamp, J.E., 1998,
358 Magnetostratigraphy-based astronomical tuning of the early Pliocene lacustrine sediments of Ptolemais
359 (NW Greece) and bed-to-bed correlation with the marine record: Earth and Planetary Science Letters, v.
360 164, no. 3-4, p. 535–551, doi: 10.1016/S0012-821X(98)00236-2.

361 Whipple, K.X., 2001, Fluvial landscape response time: How plausible is steady-state denudation?
362 American Journal of Science, v. 301, no. May, p. 313–325, doi: 10.2475/ajs.301.4-5.313.

363 Zachos, J.C., Shackleton, N.,J., Revenaugh, J.S., Pälike, H.,, Flower, B.P., 2001, Climate response to orbital
364 forcing across the Oligocene-Miocene boundary: Science, 292, 274-278.

365 Zeeden, C., S. R. Meyers, L. J. Lourens, and F. J. Hilgen (2015), Testing astronomically tuned age models,
366 Paleoceanography, 30, 369–383, doi:10.1002/2014PA002762.

367

368

Figure Captions

Click here to download Figure: EPSL_figure captions.docx

Figure 1. Location map of the As Pontes Basin, NW Spain. The map shows the principal structures and the locations of the bore holes and West Section.

Figure 2. Synthetic sedimentary facies model of the As Pontes Basin. Most of the terrigenous fraction was delivered from the North. Axial alluvial contributions became significant after the MSU deposition (see fig. 3). In the distal and restricted areas deposition of fines or coals occurred. The effects of the vegetation cover likely played an important role in the sedimentation dynamics of the basin. The main facies are indicated in numbers. The details of the facies distribution are further explained in Table 1.

Figure 3. A synthetic stratigraphic log of the basin (left) and stratigraphic record (right) in the western sub-basin combined with the magnetostratigraphic data is shown. A new magnetostratigraphic age model was built after revising the former study of Huerta et al. (1997). Marked changes occur in the lower part of their section, around chron C10n. The new correlation provides reliable sedimentation rates and is consistent with the *Issiodoromys minor* constraints.

Figure 4. Phase relationship determination. At the left the local magnetostratigraphy and the lithological log is shown. In the middle left, the facies record of Core MP208 is shown in the stratigraphic domain with the Gaussian band-pass filtered component in red superimposed (freq: 0.0827 cycles/m; bandwidth: 0.05). In the middle right, the borehole facies data of MP208 are shown in the time domain, using the magnetostratigraphic age model for conversion. Again the Gaussian band-pass filtered component of the 405-kyr cycle is shown. At the right, the eccentricity target curve (Laskar et al., 2004) is shown together with the filtered component isolating the 405-kyr eccentricity term. Red lines represent correlation lines that match maxima of the core data in the stratigraphic domain and maxima of the core data in the time domain, which are associated with clastic sediments, with successive 405-kyr eccentricity maxima. This is the unique correlation supported by the magnetochronologic age constraints.

Figure 5. The six cores used for the cyclostratigraphic analysis are shown from left to right. The facies variability is shown per core as thin black lines below the core headings. The lithology and polarity data is adapted from Huerta et al. (1997). Superimposed on these lines, the red curves mark the bandpass-filtered component centred at 12.07 m, with a bandwidth of 0.05 m^{-1}. The shifts from proximal to distal facies are correlated between all the cores, and finally to the West section. By means of magnetostratigraphy and the biochronological constraints, the West section is correlated to the GPTS of Gradstein et al. (2012). Horizontal (dashed) black lines indicate clastic pulses, which following the magnetostratigraphic age constraints are correlated to successive 405-kyr eccentricity maxima (Laskar et al., 2004). Horizontal grey shading indicates the extension of the distal facies from the cores to the West section. These coal-bearing seams are correlated to 405-kyr eccentricity minima. Bluish shading marks the stratigraphic intervals of the coal pits used with industrial purposes. These intervals correspond to 405-kyr eccentricity minima, within 2.4-Myr eccentricity minima.

Figure 6. Detail of the spectral analysis (using the REDFIT software) in the age domain for the interval underlying the Middle Sandstone Unit after applying a tuning based to the 405-kyr eccentricity cycle. Following the astronomical age model, the spectral analyses reveal significant peaks in the 100-kyr eccentricity frequency band, thus providing independent

evidence of a climatic forcing at a 405-kyr scale from the magnetostratigraphic age model. The high variability in sedimentation rates together with the intrinsic changes at a short eccentricity scale and below may account for a blurring of these cycles in some cores as MP222.

Figure 1_Location

Click here to download Figure: Fig_1_location.pdf

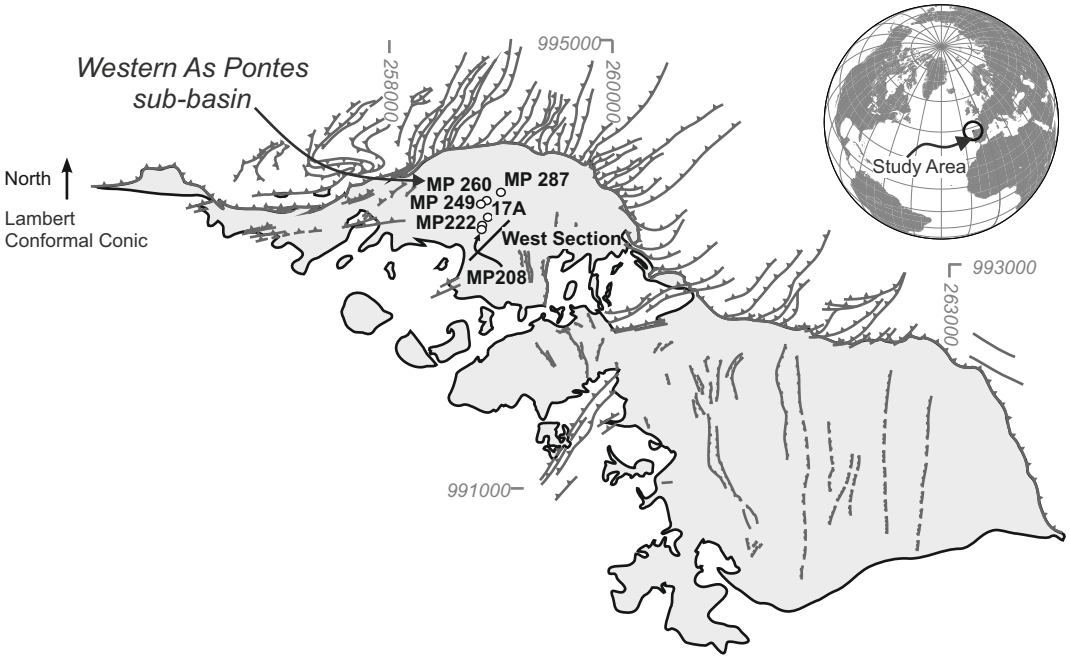

Figure 2_depos_model

Click here to download Figure: Fig_2_dep_model.pdf

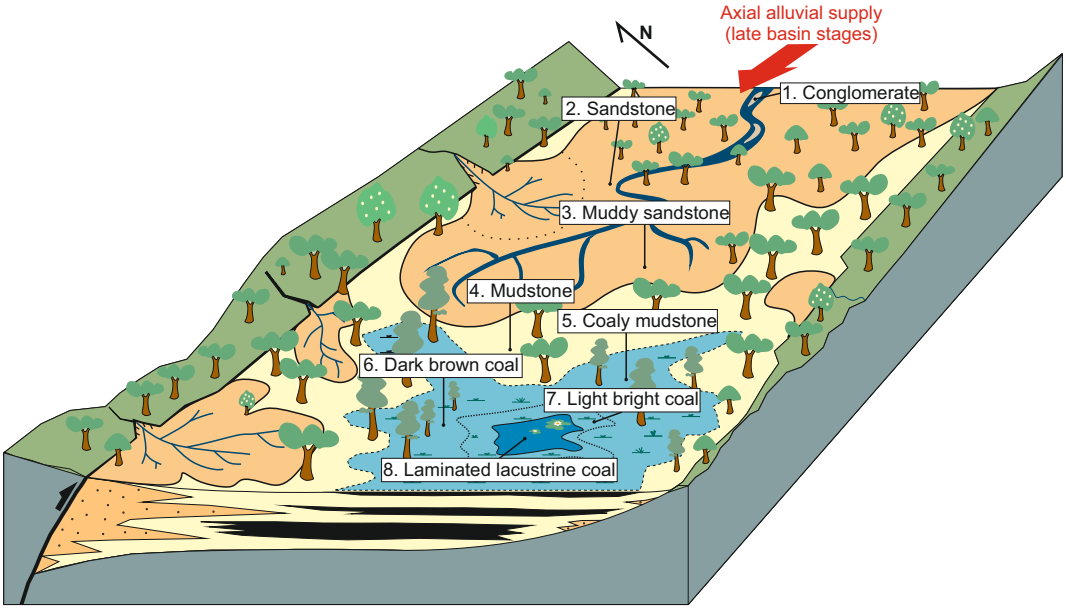

Figure 3_magnetostrat

Click here to download Figure: Fig_3_magneto.pdf

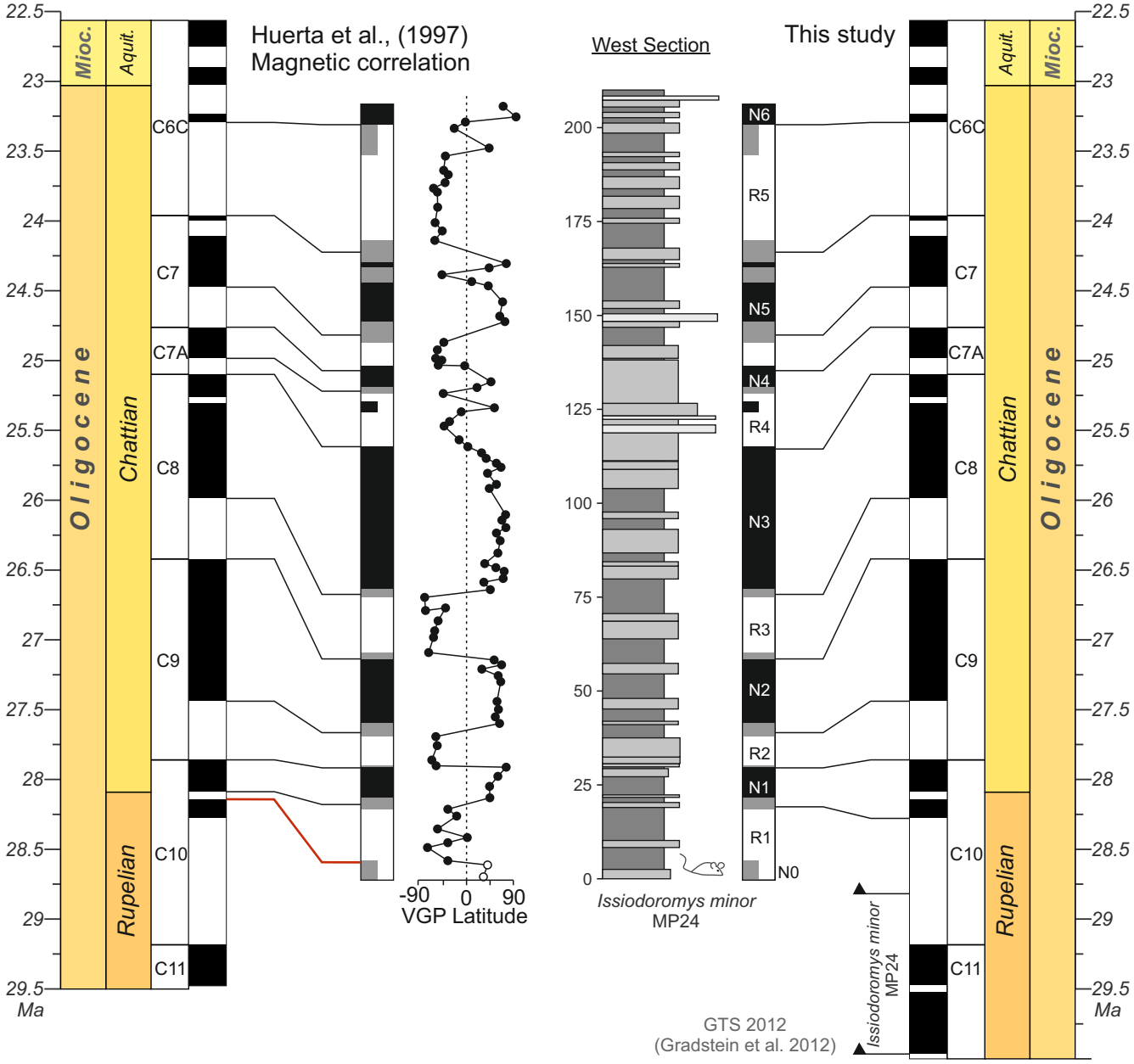

Figure 4_phase_relation

Click here to download Figure: Fig_4_phase relationship 405.pdf

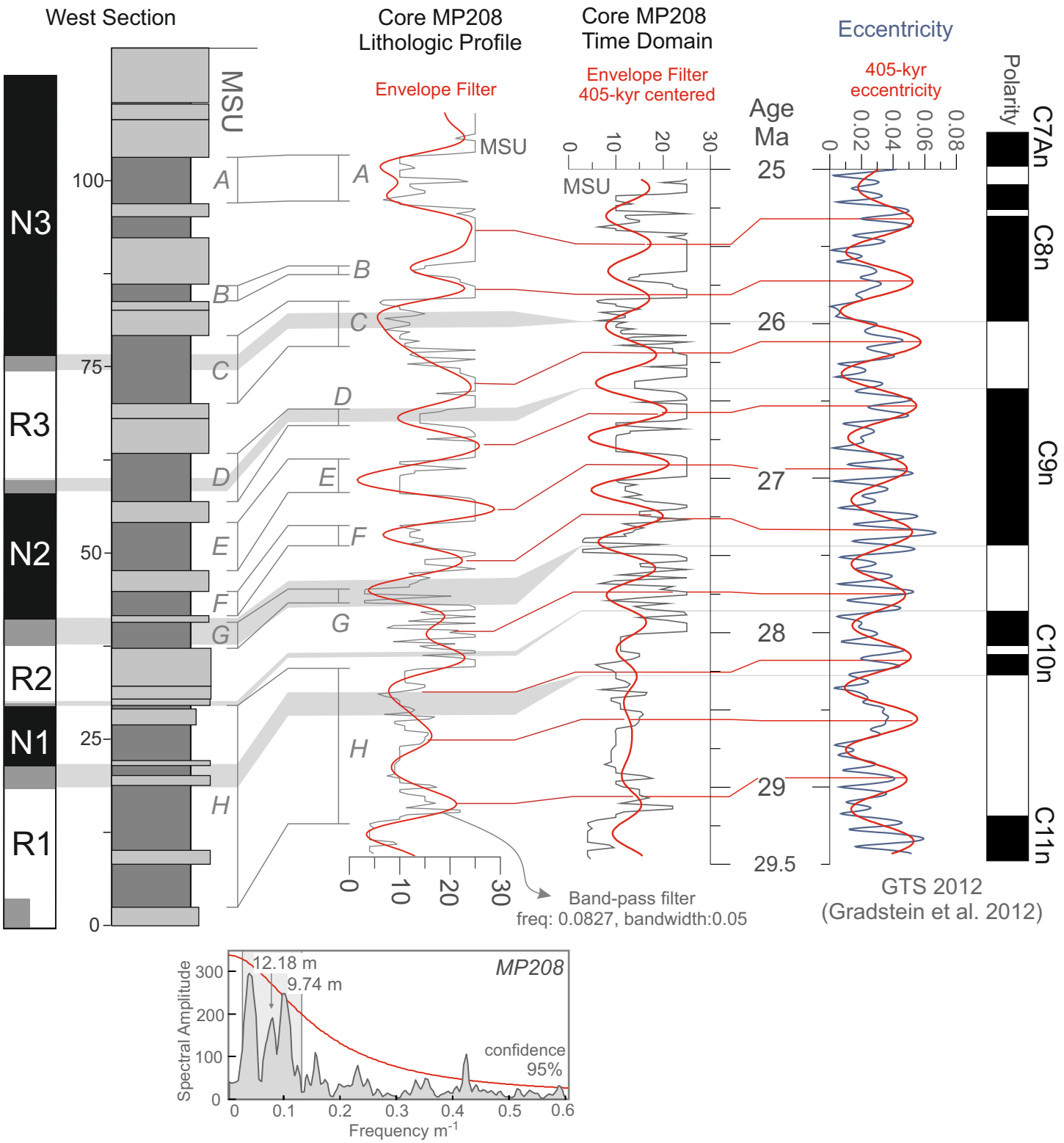

Figure 5_astrochrono

Click here to download Figure: Fig_5_correlation.pdf

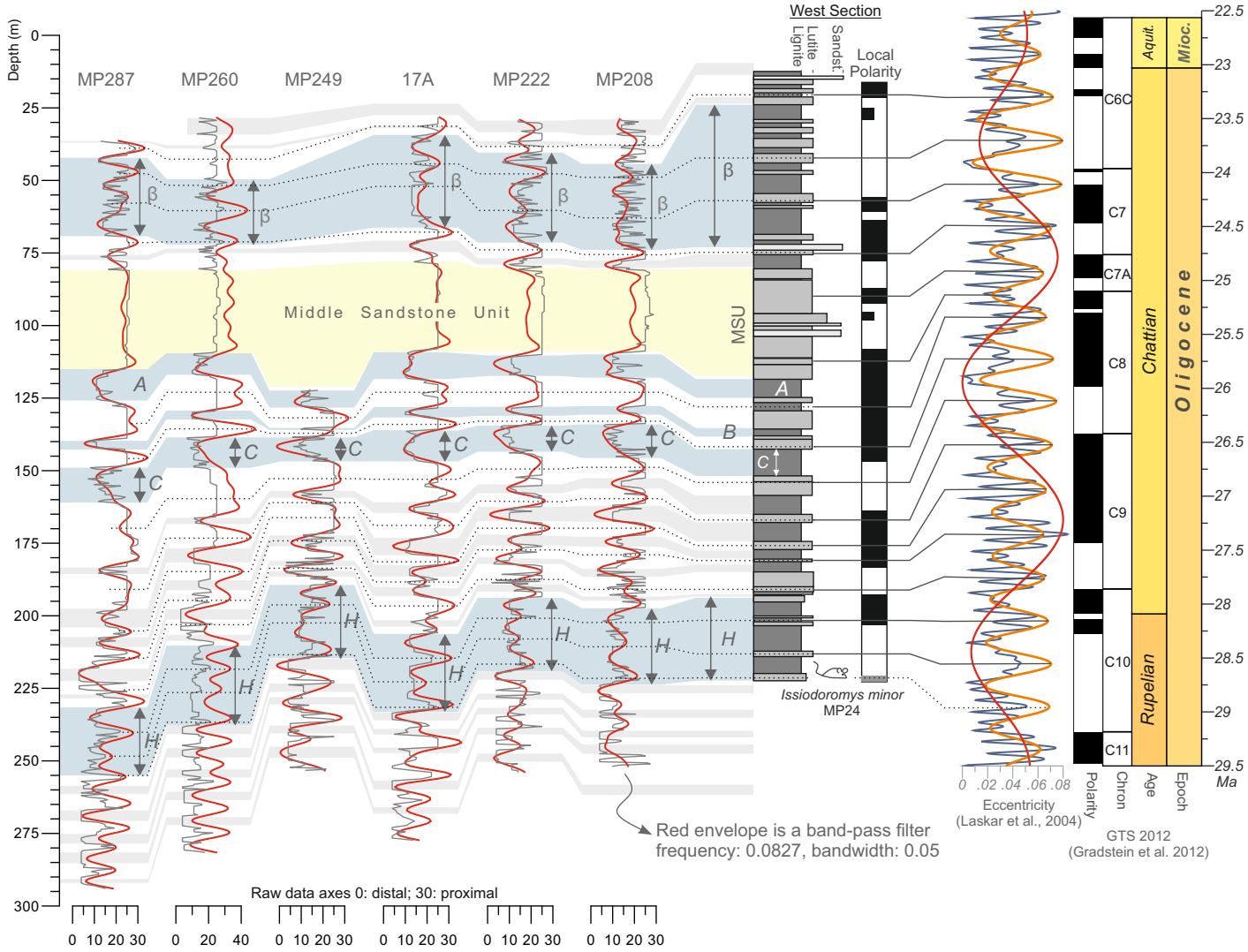

Figure 6_spectra

Click here to download Figure: Fig_6_ det_100ka.pdf

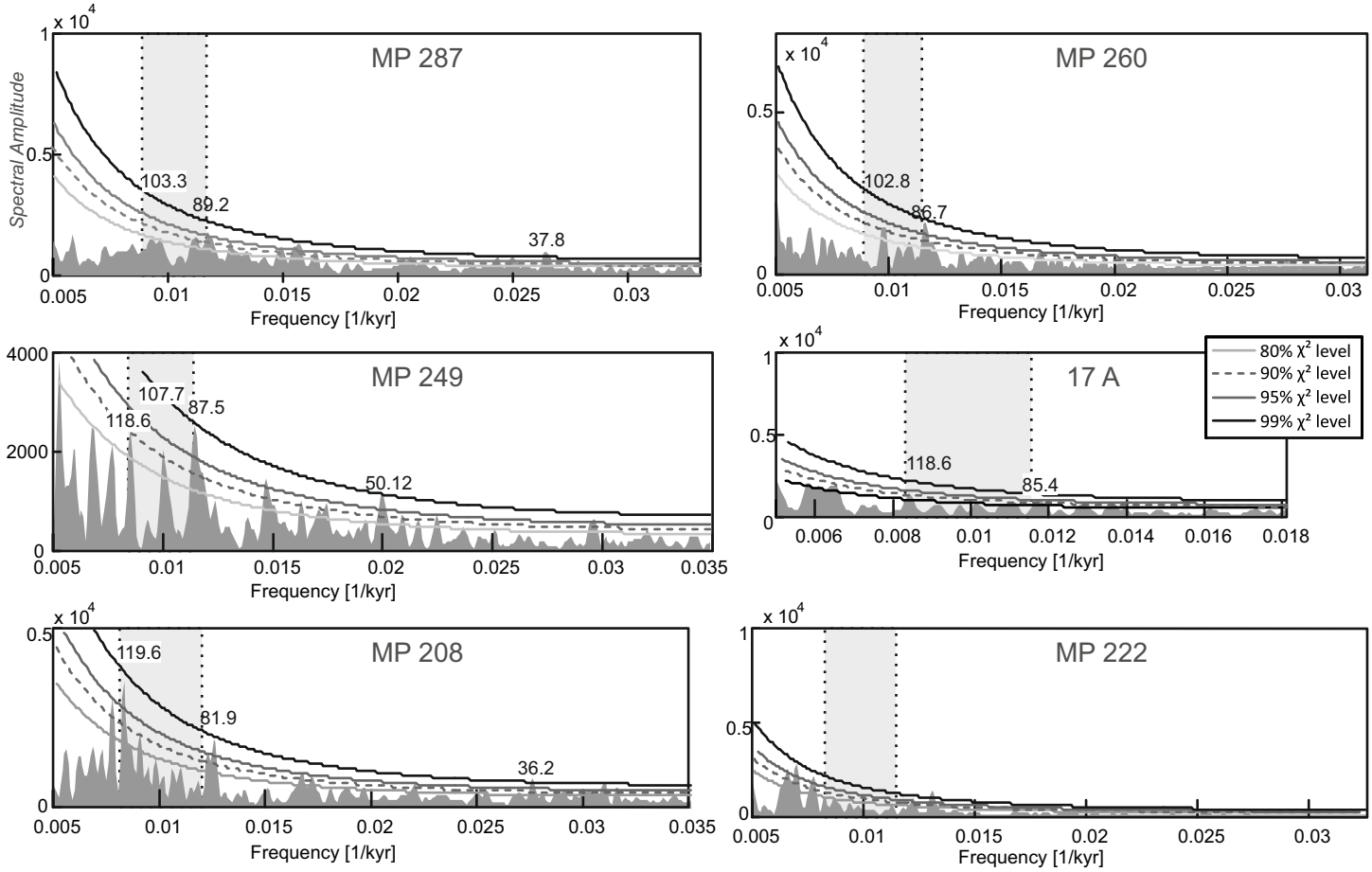

Table 1_facies rank

Click here to download Table: Table 1_Facies_rank.xlsx

Core description	Lithology	Location Fig. 2	Rank value
LAM	Laminites	8	1
LCTO	laminated lacustrine Lignite	8	2
ALC	laminated coaly lacustrine Mudstone	8	3
ALV	Green laminated Mudstone	8	4
MACICL	Green marls	8	5
PP	Light bright coal	7	6
PP..a	Light bright coal with very low mud content	7	6
PP.a	Light bright coal with low mud content	7	7
PP'a	Mud bearing Light bright coal	7	8
PPa	Muddy Light bright coal	7	9
L	Dark brown coal	6	10
L..a	Dark brown coal with very low mud	6	11
L.a	Dark brown coal with low mud content	6	12
L'a	Dark brown coal with mud	6	13
La	Muddy dark brown coal	6	14
LX	Xyloid Lignite	6	15
LX..a	Xyloid Lignite with very low mud	6	16
LX.a	Xyloid Lignite with low mud	6	17
LX'a	Xyloid Lignite with mud	6	18
LXa	Muddy Xyloid Lignite	6	19
L+A	Mudstones and Lignites	6	20
Ac	Coaly Mudstone	5	21
A'c	Mudstone with coal	5	22
A.c	Mudstone with low coal content	5	23
A..c	Mudstone with very low lignite content	5	24
A	Mudstone	4	25
A..ar	Mudstone with very low sand	3	26
A.ar	Mudstone with low sand	3	27
A'ar	Sandy Mudstone	3	28
Aar	Sandy Mudstone	3	29
S	Silt	3	30
AR'a	Sandstone with abundant mud	2	31
ANa	Muddy sandstone	2	32
AN.a	Sandstone with low mud content	2	33
AR..a	Sandstone with very low mud content	2	34
AN	Sandstone	2	35
AR'q	Quarzitic Sandstone	2	35
GRar	Sandy gravel	1	36
GRa	Muddy gravel	1	36
GR	Gravel	1	36
CG	Conglomerate	1	36
Q	Quartzite	0	x
P	Hercynian basement	0	x

Supplementary material for online publication only

Click here to download Supplementary material for online publication only: S_Fig_1_Spectrum_thickness.pdf

Supplementary material for online publication only

Click here to download Supplementary material for online publication only: S_Table_1_core_location.xlsx

Supplementary material for online publication only

Click here to download Supplementary material for online publication only: Supp_fig_captions.docx